Available online at www.sciencedirect.com
SCIENCE DIRECT®
Journal of Solid State Chemistry 175 (2003) 299–305
JOURNAL OF SOLID STATE CHEMISTRY
http://elsevier.com/locate/jssc

Synthesis and structural characterization of $Ba(Ln^{III}_{2/3}B^{VI}_{1/3})O_3$ (Ln^{III} = Dy, Gd and Sm; B^{VI} = Mo or W) complex perovskites

Antonio F. Fuentes,[a,*] M. Garza-García,[a] J.I. Escalante-García,[a] G. Mendoza-Suárez,[a] Khalid Boulahya,[b] and U. Amador[c]

[a] *CINVESTAV-IPN Unidad Saltillo, Apartado Postal 663, 25000 Saltillo, Coahuila, Mexico*
[b] *Departamento de Química Inorgánica, Facultad de Ciencias Químicas, Universidad Complutense, 28040 Madrid, Spain*
[c] *Departamento de CC. Químicas, Facultad de Ciencias Experimentales y de la Salud, Universidad San Pablo-CEU, Urbanización Montepríncipe, 28668 Boadilla del Monte, Madrid, Spain*

Received 31 January 2003; received in revised form 28 April 2003; accepted 16 May 2003

Abstract

We describe in this work the synthesis and crystal structure of five rare earth and Mo(VI) or W(VI) containing complex perovskites. The compounds studied are $Ba(Dy_{2/3}Mo_{1/3})O_3$, $Ba(Dy_{2/3}W_{1/3})O_3$, $Ba(Gd_{2/3}Mo_{1/3})O_3$, $Ba(Gd_{2/3}W_{1/3})O_3$ and $Ba(Sm_{2/3}W_{1/3})O_3$ and were prepared starting from solutions, by the polymeric precursors method. Structural characterization by HREM, SAED and powder XRD revealed the five compounds to be ordered cubic perovskites, SG *Fm*-3*m* (225), with a cell parameter double of that of a simple perovskite cell and increasing as the size of the trivalent lanthanide ion increases (Dy < Gd < Sm).

Keywords: Complex perovskites; Tungsten; Molybdenum; Lanthanides; SAED; HREM; XRD

1. Introduction

Hexavalent elements such as Mo(VI) and W(VI) can be stabilized in complex $A_nB_nO_{3n}$ perovskites, where they share the *B*-octahedrally coordinated position with another element in a lower oxidation state (e.g., 2+ in double perovskites, $A(B^{2+}_{1/2}B^{6+}_{1/2})O_3$). Compounds of this type, containing twice as much of the lower as the higher oxidation state element, are represented as $A(B'_{2/3}B''_{1/3})O_3$. Probably one of the first compounds of this type reported in literature was that of molecular formula $Ba(Sc_{2/3}W_{1/3})O_3$ [1] with an ordered cubic structure, SG *Fm*-3*m* (225), and a doubled a_p unit cell parameter (8.24 Å). It was suggested that the chemical formula of this ordered perovskite could be written as $Ba[Sc_{1/2}(Sc_{1/6}W_{1/3})]O_3$, with Sc^{3+} ions fully occupying one of the two octahedral sites available and the W^{6+} ions and the remaining Sc^{3+} ions, statistically distributed over the second octahedral site. It is well known that ordering in these complex oxides is favored first, by large differences in charge and secondly, by large differences in size between the two ions in octahedral coordination [2]. According to Galasso [3], it is the ratio $\sigma = (r_{B'} - r_{B''})/r_{B'}$ the one that determines ordering in complex perovskite crystal structures. Thus, an ordered distribution of cations should be expected for $A(B'^{3+}_{1/2}B''^{5+}_{1/2})O_3$ complex perovskites when σ values are larger than 0.09. Ionization potentials [4], cation coordination geometry and the *A*-cation/*B*-cation size ratio [5] have been also mentioned as factors determining the degree of ordering (disordering) in this type of compounds. In a recent work carried out in this group with different hexavalent tungsten and molybdenum complex perovskites, it was found that in opposition to what one would have expected from those criteria mentioned above, indium containing oxides present a random distribution of In(III) and W(VI) (or Mo(VI)) over the octahedral site. In fact, while $Ba(In_{2/3}Mo_{1/3})O_3$ presents at room temperature, a disordered structure with cubic symmetry (SG *Pm*-3*m*), $Sr(In_{2/3}W_{1/3})O_3$ was found to be orthorhombic (SG *Pnma*) and $Ba(In_{2/3}W_{1/3})O_3$ a mixture of two forms, one ordered (SG *Fm*-3*m*) and another one disordered

*Corresponding author. Fax: +52-844-4389610.
E-mail address: afernand@saltillo.cinvestav.mx (A.F. Fuentes).

0022-4596/03/$ - see front matter © 2003 Elsevier Inc. All rights reserved.
doi:10.1016/S0022-4596(03)00291-3

(SG *Pm*-3*m*) [6]. Bearing this in mind is that we decided to explore some other similar complex oxides. To the best of our understanding, it is the first time that the $Ba(Dy_{2/3}Mo_{1/3})O_3$ has ever been prepared while structural information available about the rest is difficult to find and confusing. The method selected for preparing the oxides studied in this work is the polymeric precursors method already successfully used for preparing polycation oxides with a perovskite-like structure. Starting from solution, the polymeric precursors method should lead to a more homogeneous mixing and higher reactivity of the starting reagents minimising phase segregation compare to the traditional solid-state reaction.

2. Experimental

The synthesis of the title compounds was carried out starting from the following chemical reagents: barium carbonate ($BaCO_3$, 99.98%), hydrated metal nitrates $Ln(NO_3)_3$ (Ln = Dy, Gd and Sm, 99.9%), ammonium dimolybdate and ammonium tungsten oxide, $(NH_4)_{10}W_{12}O_{41} \cdot 5H_2O$ (99.999%). Commercially available ammonium dimolybdate was found to be a mixture of different molybdenum salts. Therefore, it was thermally decomposed to yield pure MoO_3 so that its molybdenum content could be determined. The remaining chemicals were used as supplied by the manufacturers. Starting reagents were dissolved in an aqueous citric acid (CA, 99.5%) solution under constant stirring. After a moderate heating to obtain clear solutions, ethylene glycol (EG, 99 + %) was added to promote polymerization of the metal citrates by a polyesterification reaction (CA/EG molar ratio = 1). After heating the solutions to $\sim$100°C to evaporate water molecules, gels of high viscosity were obtained which on turn, were dried at 150°C/5 h yielding solid resins of high porosity. After grinding, these powdered precursors were subjected to different thermal treatments in high alumina crucibles (Adolph Coors, Inc.) by using an electrical furnace.

Chemical reactions were followed by X-ray powder diffraction (XRD) on a Philips X'Pert diffractometer with Cu$K\alpha$ radiation (1.5418 Å) and nickel filter. XRD patterns were analyzed by the Rietveld method, using the FULLPROF program [7].

Samples were also characterized by SAED and HREM in a PHILIPS CM200 FEG electron microscope, fitted with a double tilting goniometer stage ($\pm$40°, $\pm$24°). Local cationic composition was determined by energy-dispersive X-ray spectroscopy (EDS) with an EDAX analyser system attached to the above-mentioned microscope. Simulated HREM images were calculated by the multislice method using the MacTempas software package.

Thermal analysis were carried out in a Perkin-Elmer TGA 7/PC and a Perkin-Elmer TAC/DX using a typical sample size of approximately 10 mg, a heating rate of 10°C/min and a static air atmosphere.

3. Results and discussion

3.1. Synthesis

Firing the solid resins at 1200°C (heating rate 10°C/min), produced a powder composed primarily by a phase with an XRD diffraction pattern similar to that of a perovskite. Barium tungstates and molybdates of different stoichiometry or the oxides of the trivalent lanthanides (Gd_2O_3, Dy_2O_3 or Sm_2O_3) were also present in some samples as minor impurities. All powders were subjected to further firings until the complete removal of

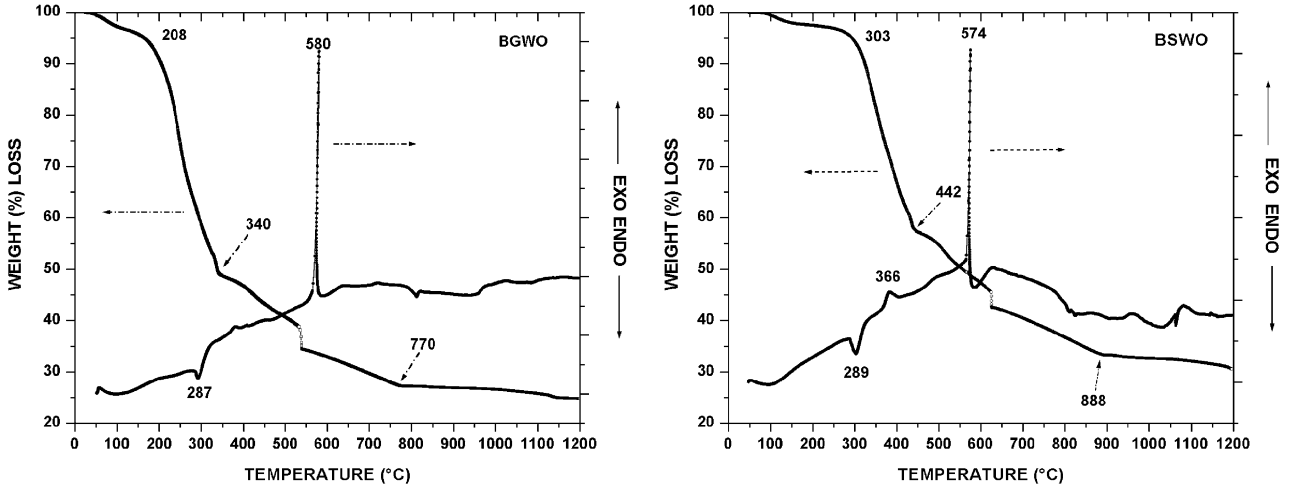

Fig. 1. TGA-DTA curves corresponding to samples $Ba(Gd_{2/3}W_{1/3})O_3$ and $Ba(Sm_{2/3}W_{1/3})O_3$.

undesired phases or until no changes were observed in the diffraction patterns collected after two consecutive thermal treatments assuming then, that the system was at equilibrium. The color of the powder was found to depend on both, the hexavalent and the rare earth present. Thus, $Ba(Gd_{2/3}W_{1/3})O_3$ and $Ba(Sm_{2/3}W_{1/3})O_3$ powders were white, $Ba(Gd_{2/3}Mo_{1/3})O_3$ powder was yellow, $Ba(Dy_{2/3}W_{1/3})O_3$ dark gray and $Ba(Dy_{2/3}Mo_{1/3})O_3$ brown. A precursor mixture prepared with barium, samarium and molybdenum yielded a mixture of several phases which, despite further long thermal treatments at high temperatures, never evolved into a perovskite-like compound.

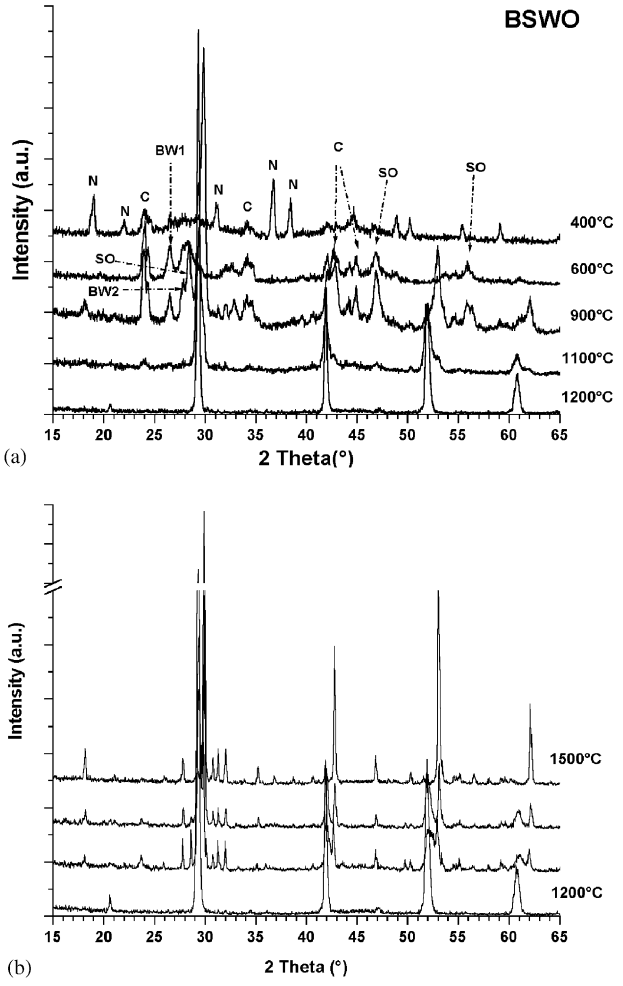

Fig. 2. XRD study of the evolution of $Ba(Sm_{2/3}W_{1/3})O_3$ with temperature between 400°C and 1100°C (a) and between 1200°C and 1500°C (b).

Portions of the five resins were treated at different temperatures and characterized by thermal analysis and XRD. Since all the resins showed many similarities in their thermal behavior, only two selected examples will be shown here. Thus, Fig. 1 shows TGA-DTA curves for $Ba(Gd_{2/3}W_{1/3})O_3$ and $Ba(Sm_{2/3}W_{1/3})O$. From them, it is clear that the majority of the chemical reactions involving weight losses, such as decomposition of the organic polymeric network with evolution of CO_2 and H_2O, were completed below 600°C. The end of this process is marked in the DTA curves by the presence of an important exothermic event. Above this temperature, an additional and almost continuous, 12% weight loss is observed, most of it below 900°C suggesting the presence of carbonates. A powder XRD study of the evolution of all the five precursors with temperature, showed many similarities. $Ba(NO_3)_2$ and $BaCO_3$ were the only crystalline species observed below 500°C suggesting that barium atoms are freed during the initial stages of the polymeric network decomposition. Firing between 500°C and 600°C brings about the decomposition of $Ba(NO_3)_2$ and the formation of $BaMO_4$ (M = Mo or W). Thermal treatments between 600°C and 900°C do not produce important changes in the number or nature of phases present while firing above this latter temperature brings about the formation of a perovskite-like phase. Fig. 2 shows an XRD study of the evolution of the $Ba(Sm_{2/3}W_{1/3})O_3$ precursor with temperature between 400 and 1100°C (Fig. 2(a)) and between 1200°C and 1500°C (Fig. 2(a)). The powder pattern obtained for the precursor fired for 1 h at 400°C shows the presence of barium carbonate and nitrate as the only crystalline phases. Increasing the firing temperature to 600°C brings about the formation of $BaWO_4$ and possibly Sm_2O_3. Further heating at 1200°C

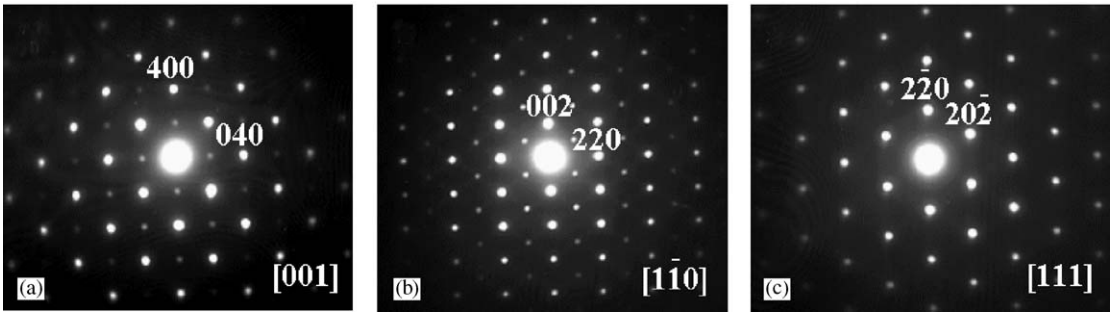

Fig. 3. SAED patterns corresponding to $Ba(Dy_{2/3}Mo_{1/3})O_3$, taken along [001] (a), [1$\bar{1}$0] (b) and [111] (c).

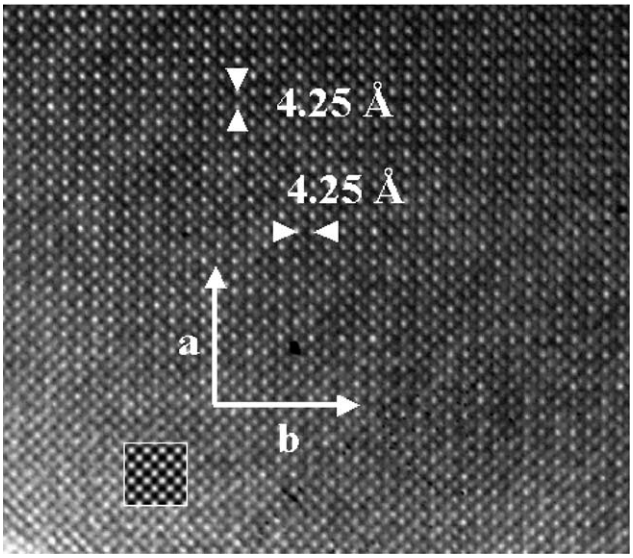

Fig. 4. HREM corresponding to $Ba(Dy_{2/3}Mo_{1/3})O_3$, taken along [001]. Simulated image at $\Delta t = 4$ nm and $\Delta f = -45$ nm is shown at the inset.

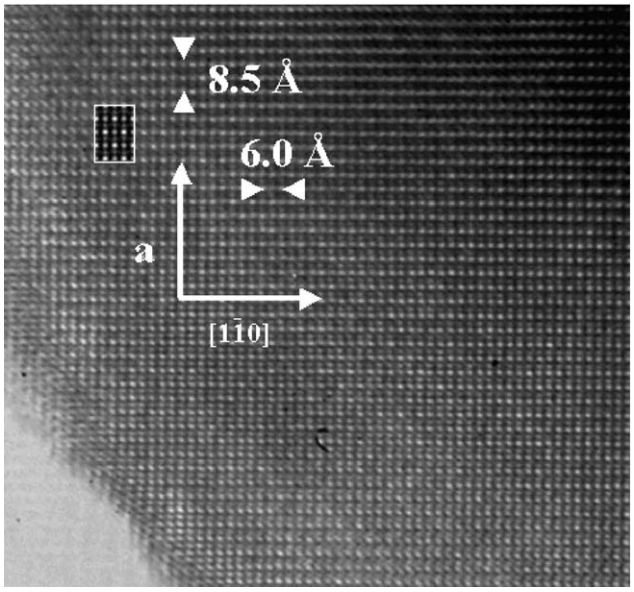

Fig. 5. HREM corresponding to $Ba(Dy_{2/3}Mo_{1/3})O_3$, taken along [1$\bar{1}$0]. Simulated image at $\Delta t = 8$ nm and $\Delta f = -65$ nm is shown at the inset.

produces a powder with a X-ray diffraction pattern typical of a perovskite-like phase while heating the powder at higher temperatures, leads to the decomposition of $Ba(Sm_{2/3}W_{1/3})O_3$ as evidenced by the presence of the characteristic reflections of monoclinic Sm_2O_3. In addition to this phase, a series of sharp reflections were also observed which could not be assigned to any known phase. There is a triclinic form of a barium tungstate, Ba_3WO_6 [8], which presents a similar pattern though shifted towards lower 2θ values. Further work is currently being carried out on this phase to fully characterize its chemical composition and structure.

3.2. Structural analysis

The Goldschmidt tolerance factor values calculated for the title compounds fall between 0.951 for the Sm containing phase and 0.965 for that with Dy and Mo, suggesting that all of them should be cubic with a structure close to that of an ideal perovskite. These values were calculated by using the formula given by Goldschmidt and the ionic radii given by Shannon [9]. A weighed mean was used for the ionic radii of the elements in octahedral coordination calculated as follows: $R_B = (2R_{B(\mathrm{III})} + R_{B(\mathrm{VI})})/3$. After a literature review, we found only a few papers dealing with similar compounds. Thus, Galasso claimed to have synthesized $Ba(Dy_{2/3}W_{1/3})O_3$ and $Ba(Gd_{2/3}W_{1/3})O_3$ and proposed for them a $(NH_4)_3FeF_6$-like structure with cell parameters of 8.386 and 8.411 Å, respectively [3].

Hikichi and Suzuki [10] studied several barium and tungsten containing perovskites including that with Dy and W. According to their published work, pure cubic $Ba(Dy_{2/3}W_{1/3})O_3$ was obtained after heating a stoichiometric mixture of WO_3, Dy_2O_3 and $BaCO_3$ 48 h at 1300°C. In opposition to Galasso's work [3], they mentioned that since no superlattice lines could be observed in the powder XRD pattern even after firing the sample at temperatures of 1500°C, the distribution of Dy and W over the octahedral site should be random with $a = 4.264$ Å. However, small difference in atomic scattering factor between Dy and W was mentioned as

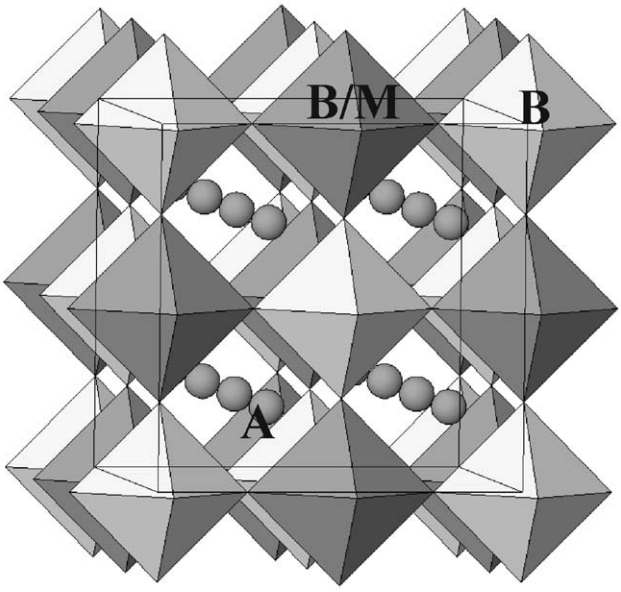

Fig. 6. Schematic representation of the structure of a cubic perovskite with unit cell $2a_p \times 2a_p \times 2a_p$ originated by the ordering of the cations in octahedral coordination.

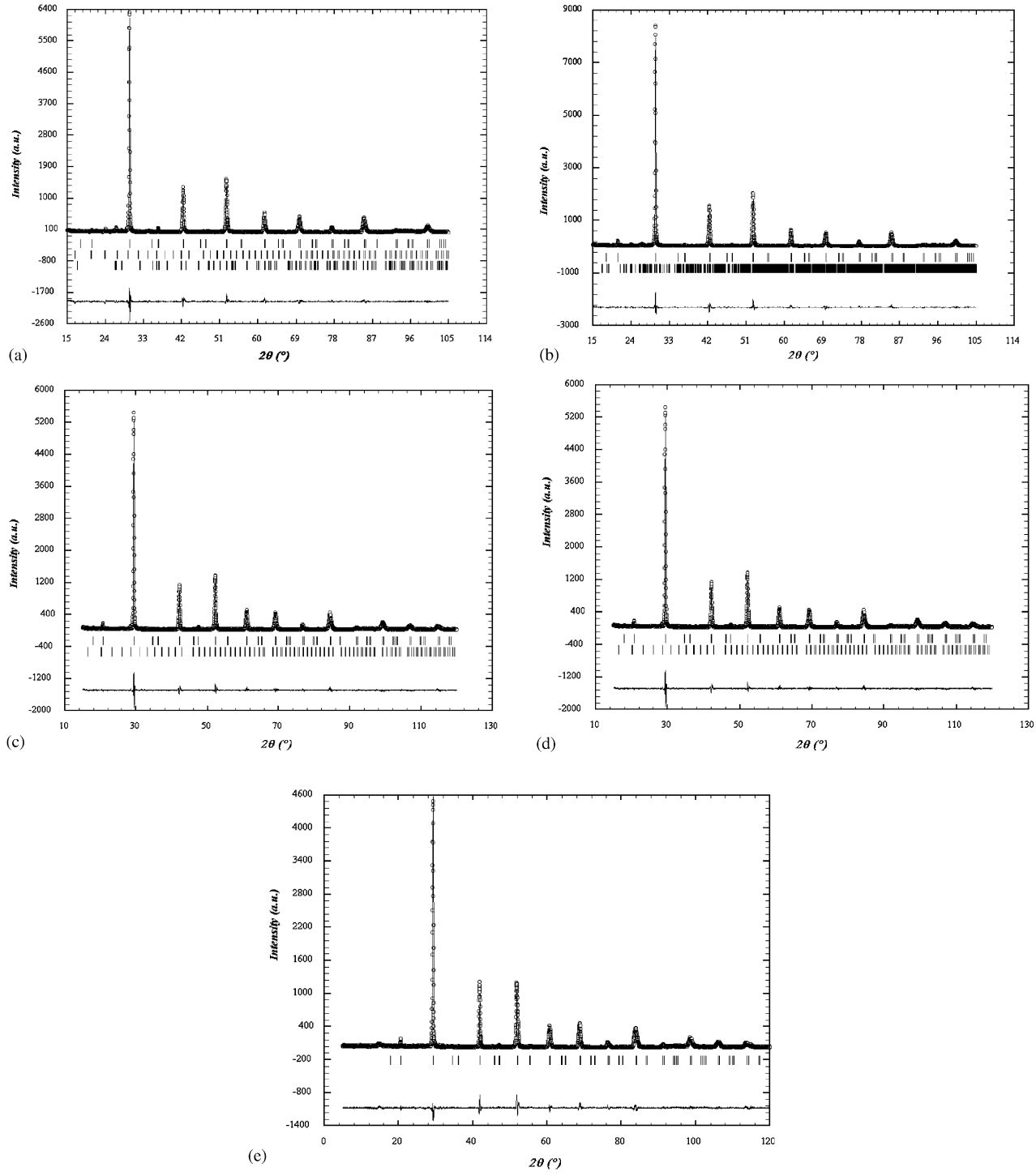

Fig. 7. (a) Experimental (circles) and calculated XRD patterns, and their difference, for $Ba(Dy_{2/3}Mo_{1/3})O_3$. Vertical marks indicate the peaks of the phases present in the sample: first row $Ba(Dy_{2/3}Mo_{1/3})O_3$, second row Dy_2O_3, third row $BaMoO_4$. (b) Experimental (circles) and calculated XRD patterns, and their difference, for $Ba(Dy_{2/3}W_{1/3})O_3$. Vertical marks indicate the peaks of the phases present in the sample: first row $Ba(Dy_{2/3}W_{1/3})O_3$, second row $BaWO_4$. (c) Experimental (circles) and calculated XRD patterns, and their difference, for $Ba(Gd_{2/3}W_{1/3})O_3$. Vertical marks indicate the peaks of the phases present in the sample: first row $Ba(Gd_{2/3}W_{1/3})O_3$, second row Gd_2O_3.. (d) Experimental (circles) and calculated XRD patterns, and their difference, for $Ba(Gd_{2/3}Mo_{1/3})O_3$. Vertical marks indicate the peaks of the phases present in the sample: first row $Ba(Gd_{2/3}Mo_{1/3})O_3$, second row Gd_2O_3, third row $BaMoO_4$. (e) Experimental (circles) and calculated XRD patterns, and their difference, for $Ba(Sm_{2/3}W_{1/3})O_3$. Vertical marks indicate the positions of the peaks.

a possible reason for not being able to observe ordering by XRD powder diffraction.

In our case and since the sole use of the XRD patterns does not allow developing a complete structural model, the complementary information provided by electron diffraction was also used. Selected area electron diffraction (SAED) was used to fully reconstruct the reciprocal space for the title compounds finding out that all of them belonged to the same type of structure. Thus, as an example, in Fig. 3 the most relevant zone axes, the [100], [1$\bar{1}$0] and [111] ones, corresponding to $Ba(Dy_{2/3}Mo_{1/3})O_3$, are depicted. All maxima can be indexed in double cubic perovskite unit cell and the reflection conditions found are compatible with the *Fm*-3*m* space group, previously proposed for other double cubic perovskites, such as Ba_2PtPrO_6 [11].

On the other hand, HREM micrograph taken along the [001] zone axis (Fig. 4), shows an ordered material with *d*-spacings 4.25 and 4.25 Å, corresponding to $d_{2\,0\,0}$ and $d_{0\,2\,0}$ according to the above described unit cell. The contrast variation observed in this micrograph is characteristic of a simple perovskite. However, the most informative HREM micrograph taken along the [1$\bar{1}$0] zone axis (Fig. 5), shows an apparently well ordered material with *d*-spacings 6.0 and 8.5 Å, corresponding to $d_{1\,1\,0}$ and $d_{0\,0\,1}$ according to the above described unit cell. The contrast variation corresponds to bright dots alternating with less bright ones along both directions. Such contrast is the one characteristic of double perovskites. Therefore, from the refined atomic coordinates of $Ba(Dy_{2/3}Mo_{1/3})O_3$ (see the next section), an image calculation was performed. The simulated images fits nicely to the experimental ones (inset of Figs. 4 and 5).

The structural model used to fit the experimental XRD data was developed on the basis of the SAED and HREM results described above, a schematic representation of it is shown in Fig. 6. Fig. 7 depicts observed, calculated and difference powder diffraction patterns for the title compounds. Tick marks indicate in every case the reflection positions for both, the perovskites and impurity phases. The corresponding structural parameters are collected in Table 1, whereas Table 2 shows some selected inter-atomic distances.

As expected, the five compounds presented in this paper were found to present an ordered distribution of Ln^{3+} and hexavalent W (or Mo) over the octahedral sites. Large differences in charge (+3) and ionic radii ($\Delta R > 0.3$ Å) drive these crystal structures towards and ordered state.

Table 1
Final structural parameters of $Ba(Ln_{2/3}B_{1/3})O_3$ compounds

Atom	Ba	Ln^{3+}	Ln^{3+}/B^{6+}	O(1)
$Ba(Dy_{2/3}Mo_{1/3})O_3$[a]				
x/*a*	1/4	0	1/2	0.267(2)
y/*b*	1/4	0	1/2	0
z/*c*	1/4	0	1/2	0
B_{iso} (Å^2)	0.56(8)	0.58(9)	0.59(6)	2.4(3)
Occ	1	3/6	1/6:2/6	3
$Ba(Dy_{2/3}W_{1/3})O_3$[b]				
x/*a*	1/4	0	1/2	0.236(3)
y/*b*	1/4	0	1/2	0
z/*c*	1/4	0	1/2	0
B_{iso} (Å^2)	0.47(4)	1.75(7)	1.70(6)	2.7(6)
Occ	1	3/6	1/6:2/6	3
$Ba(Gd_{2/3}W_{1/3})O_3$[c]				
x/*a*	1/4	0	1/2	0.238(2)
y/*b*	1/4	0	1/2	0
z/*c*	1/4	0	1/2	0
B_{iso} (Å^2)	0.77(6)	0.44(5)	0.47(6)	3.2(6)
Occ	1	3/6	1/6:2/6	3
$Ba(Gd_{2/3}Mo_{1/3})O_3$[d]				
x/*a*	1/4	0	1/2	0.257(5)
y/*b*	1/4	0	1/2	0
z/*c*	1/4	0	1/2	0
B_{iso} (Å^2)	1.00(3)	0.79(2)	0.81(4)	3.4(6)
Occ	1	3/6	1/6:2/6	3
$Ba(Sm_{2/3}W_{1/3})O_3$[e]				
x/*a*	1/4	0	1/2	0.249(3)
y/*b*	1/4	0	1/2	0
z/*c*	1/4	0	1/2	0
B_{iso} (Å^2)	0.41(4)	0.10(5)	0.21(6)	3.3(8)
Occ	1	3/6	1/6:2/6	3

[a] For $Ba(Dy_{2/3}Mo_{1/3})O_3$, SG *Fm*-3*m* (n. 225), $a = 8.5278(3)$ Å, $V = 620.17(4)$ Å^3, $R_B = 0.03$, $R_{exp} = 0.112$, $R_{wp} = 0.169$, $\chi^2 = 2.1$.
[b] For $Ba(Dy_{2/3}W_{1/3})O_3$, SG *Fm*-3*m* (n. 225), $a = 8.5276(3)$ Å, $V = 620.14(3)$ Å^3, $R_B = 0.029$, $R_{exp} = 0.110$, $R_{wp} = 0.148$, $\chi^2 = 1.8$.
[c] For $Ba(Gd_{2/3}W_{1/3})O_3$, SG *Fm*-3*m* (n. 225), $a = 8.5817(3)$ Å, $V = 632.00(3)$ Å^3, $R_B = 0.04$, $R_{exp} = 0.120$, $R_{wp} = 0.147$, $\chi^2 = 1.5$.
[d] For $Ba(Gd_{2/3}Mo_{1/3})O_3$, SG *Fm*-3*m* (n. 225), $a = 8.5794(5)$ Å, $V = 631.49(6)$ Å^3, $R_B = 0.05$, $R_{exp} = 0.128$, $R_{wp} = 0.146$, $\chi^2 = 1.3$.
[e] For $Ba(Sm_{2/3}W_{1/3})O_3$, SG *Fm*-3*m* (n. 225), $a = 8.6226(3)$ Å, $V = 641.09(4)$ Å^3, $R_B = 0.08$, $R_{exp} = 0.129$, $R_{wp} = 0.171$, $\chi^2 = 1.8$.

4. Concluding remarks

Five $Ba(Ln^{3+}_{2/3}B^{6+}_{1/3})O_3$ (Ln^{3+} = Dy, Gd and Sm; B^{6+} = Mo and W) were prepared by the polymeric precursors method and characterized by HREM, SAED and powder XRD. Barium carbonate and nitrate as well as barium tungstates and molybdates of different stoichiometry were observed after firing the solid resin at temperatures higher than 400°C. As expected, SAED and HREM showed all five compounds to be ordered cubic complex perovskites, SG *Fm*-3*m*. Large differences in charge and size between Mo^{6+} or W^{6+} and Ln^{3+}, both in octahedral coordination, drives these structures towards an ordered distribution of cations. Having both hexavalent cations, Mo^{6+} and W^{6+}, in octahedral coordination, similar ionic radii, 0.59 vs.

Table 2
Selected inter-atomic distances (Å) in $Ba(Ln^{3+}_{2/3}B^{6+}_{1/3})O_3$ compounds

$Ba(Dy_{2/3}Mo_{1/3})O_3$		$Ba(Dy_{2/3}W_{1/3})O_3$		$Ba(Gd_{2/3}W_{1/3})O_3$		$Ba(Gd_{2/3}Mo_{1/3})O_3$		$Ba(Sm_{2/3}W_{1/3})O_3$	
Ba–O	$3.02(1)\times 12$	Ba–O	$3.02(1)\times 12$	Ba–O	$3.04(1)\times 12$	Ba–O	$3.03(1)\times 12$	Ba–O	$3.05(2)\times 12$
Dy–O	$2.28(2)\times 6$	Dy–O	$2.01(2)\times 6$	Gd–O	$2.04(2)\times 6$	Gd–O	$2.21(4)\times 6$	Sm–O	$2.14(2)\times 6$
Dy/Mo–O	$1.99(2)\times 6$	Dy/W–O	$2.25(2)\times 6$	Gd/W–O	$2.25(2)\times 6$	Gd/Mo–O	$2.08(4)\times 6$	Sm/W–O	$2.17(2)\times 6$

0.60 Å [9], cell size depends on the size of the rare earth element an increases linearly with the ionic radius of Ln^{3+}.

Acknowledgments

Financial assistance from CONACYT (Mexico) is gratefully acknowledged (Grant 31198U).

References

[1] F.J. Fresia, L. Katz, R. Ward, J. Am. Chem. Soc. 81 (1959) 4783.
[2] F.K. Patterson, C.W. Moeller, R. Ward, Inorg. Chem. 2 (1963) 196.
[3] F.S. Galasso, Structure, Properties and Preparation of Perovskite-Type Compounds, Pergamon Press, Oxford, 1969.
[4] A.A. Bokov, N.P. Protsenko, Z.-G. Ye, J. Phys. Chem. Solids 61 (2000) 1519.
[5] M.T. Anderson, K.B. Greenwood, G.A. Taylor, K.R. Poeppelmeier, Prog. Solid State Chem. 22 (1993) 197.
[6] A.F. Fuentes, O. Hernadez-Ibarra, J.I. Escalante-Garcia, G. Mendoza-Suarez, K. Boulahya, U. Amador, J. Solid State Chem. 173 (2003) 319.
[7] J. Rodriguez-Carvajal, FULLPROF program, in: Abstracts of the Satellite Meeting on Powder Diffraction of the XVth Congress of the IUCr, Toulouse, France, 1990, p. 17.
[8] V.L. Balashov, A.A. Kharlanov, O.I. Kondratov, V.V. Fomichev, Zh. Neorg. Khim. 36 (1991) 456.
[9] R.D. Shannon, Acta Crystallogr. A 32 (1976) 751.
[10] Y. Hikichi, S. Suzuki, Mater. Res. Bull. 22 (1987) 219.
[11] U. Amador, C.J.D. Hetherington, E. Moran, M.A. Alario-Franco, J. Solid State Chem. 96 (1992) 132.